Chemical Engineering Journal 148 (2009) 405–413

Contents lists available at ScienceDirect

Chemical Engineering Journal

journal homepage: www.elsevier.com/locate/cej

A centrifugation method for the assessment of low pressure compressibility of particulate suspensions

Daan Curvers[a,*], Hans Saveyn[a], Peter J. Scales[b], Paul Van der Meeren[a]

[a] Particle and Interfacial Technology Group, Faculty of Bioscience Engineering, Ghent University, 9000 Ghent, Belgium
[b] Particulate Fluids Processing Centre, University of Melbourne, Victoria, Australia

ARTICLE INFO

Article history:
Received 19 June 2008
Received in revised form 25 August 2008
Accepted 11 September 2008

Keywords:
Centrifugation
Modelling
Sludge
Dewatering
Filtration
Compressibility

ABSTRACT

This work describes an easy methodology for assessing the compressibility of particulate suspensions at relatively low pressures. The material used in this study was an anaerobically digested waste water sludge. Using a centrifuge, the equilibrium sediment bed height was recorded as a function of rotational speed during the centrifugation. This approach avoids errors due to expansion of the sediment bed after the centrifugation is stopped, a phenomenon typically seen with waste water sludges. A straightforward numerical method was used to solve a one-dimensional centrifugation model describing the equilibrium sediment bed height as a function of rotational speed. It has been shown that this approach yields realistic results. The one-dimensional model is able to describe the compressibility of the anaerobically digested sludge. Besides yielding a close fit for the measured sediment bed heights, extrapolating these results to a different initial solids volume fraction resulted in a good prediction of the bed height as well. Different constitutive equations for the relation between solids pressure and solids volume fraction were assessed. The typical power law functions [F. Tiller, W. Leu, Basic data fitting in filtration, Journal of the Chinese Institute of Chemical Engineers 11 (1980) 61–70], often used in filtration modelling, were the most adequate for describing the compressional behaviour of the sludge. A functional relation based on the osmotic pressure within the solids network, suggested for describing the phenomenology of filtration dewatering [K. Keiding, M. Rasmussen, Osmotic effects in sludge dewatering, Advances in Environmental Research 7 (2003) 641–645], could not be used to adequately describe the behaviour of the sludge at the low pressures generated during centrifugation.

1. Introduction

Waste water treatment produces enormous amounts of excess activated sludge and/or anaerobically digested sludges as a sidestream. Before the sludge is disposed of, the solids concentration is increased through a series of different operations in order to reduce the transportation and disposal costs [3]. With regard to dewatering, mechanical processes are economically more favourable than thermal ones [4]. The main processes used for increasing the solids concentration are gravitational thickening, centrifugation and pressure filtration. Because of the high associated costs, understanding and predicting the behaviour of these processes is of great importance to the waste water treatment industry.

The first major attempt to derive a mathematical background for describing filtration kinetics was made by Ruth in the early 1930's [5,6]. Since then, the modelling of dewatering processes has been a major topic of interest. Even though Ruth acknowledged the impact of compressibility on the solids distribution within the cake, solids were assumed to be incompressible in the earliest work. Incompressible solids lead to a filter cake with a homogeneous solids concentration and permeability that is insensitive to the applied pressure. Although the basic concepts of these theories have proven to be valid, most materials show compressible behaviour to some extent. Activated sludge, and more generally biological materials, are known to possess a very high compressibility [7,8] and a low permeability or, accordingly, a high specific resistance at moderate to high pressures. Hence, most of the mathematical models for dewatering comprise two material properties, being a compressibility term and a permeability term.

Various approaches to describing filtration behaviour start from an adapted form of the Darcy equation:

$$q = -\frac{1}{\mu\alpha}\frac{dp_s}{dx}, \quad (1)$$

* Corresponding author.
E-mail address: Daan.Curvers@UGent.be (D. Curvers).

1385-8947/$ – see front matter © 2008 Elsevier B.V. All rights reserved.
doi:10.1016/j.cej.2008.09.030

Nomenclature

List of symbols

a	acceleration [m/s^2]
A	fitting parameter in constitutive Eq. (6)
b	correction factor for solids density in Eq. (20)
B	fitting parameter in constitutive Eq. (6)
e	void ratio $= (1-\phi)/\phi$
f	number of finite differences used
F_c	centrifugal force [N]
F_x	X-component of centrifugal force [N]
F_y	Y-component of centrifugal force [N]
H	absolute height within sediment bed [m]
m	mass [kg]
n	fitting parameter in constitutive Eq. (3)
p_s	solids pressure [Pa]
p_a	fitting parameter in constitutive Eqs. (2)–(5)
P_y	compressive yield stress [Pa]
q	superficial liquid velocity [m/s]
r	hindered settling factor
$\mathcal{R}$	universal gas constant [J K^{-1} mole^{-1}]
R	radius of rotation [m]
R_{max}	radius of rotation at the bottom of the sample tube [m]
R_{top}	radius of rotation at the top of the sediment [m]
R^2	coefficient of determination
S	cross-sectional area [m^2]
SSE_{fit}	sum of squared errors between experimental values and fit [m^2]
SSE_{mean}	sum of squared errors between experimental values and experimental mean value [m^2]
T	temperature [K]
V	volume of a particle [m^3]
w	material coordinate [m]
w_{tot}	top of sediment in material coordinates [m]
x	absolute height in filter cake [m]
Δy	Euclidean distance from X-axis [m]

Greek letters

α	specific filtration resistance [1/m^2]
α_0	specific filtration resistance for $p_s = 0$ [1/m^2]
β	fitting parameter in constitutive Eqs. (2), (4), (5)
ε	porosity
γ	angular deviation from X-axis
μ	dynamic liquid viscosity [Pa s]
ϕ	solids volume fraction
ϕ_g	solids volume fraction for $p_s = 0$
ρ	density [kg/m^3]
σ	charge density [eq/kg]
ω	angular speed [rad/s]

with q the superficial liquid velocity [m/s], μ the liquid viscosity [Pa s], α the specific resistance [1/m^2], p_s the solids pressure [Pa] and x the height within the cake [m]. In pressure dewatering, the local solids pressure is the difference between the total applied pressure and the local liquid pressure. In the case of an incompressible cake, the porosity does not depend on the solids pressure, and hence the porosity and specific resistance are constant throughout the cake. In the case of a compressible system, however, an increase in solids pressure causes a decrease in porosity and an increase in specific resistance. To relate the porosity and the specific resistance to the solids pressure, different forms of constitutive equations have been suggested. The so-called power law functions proposed by Tiller and Leu [1] are probably the most widely used:

$$\phi = \phi_g \left(1 + \frac{p_s}{p_a}\right)^{\beta}, \tag{2}$$

and

$$\alpha = \alpha_0 \left(1 + \frac{p_s}{p_a}\right)^{n}. \tag{3}$$

ϕ is the solids volume fraction, equal to $(1-\varepsilon)$ with ε the porosity [−]. ϕ_g and α_0 are the volume fraction and specific resistance when the solids are in contact without being compressed ($p_s = 0$). ϕ_g is also called the gel point, as it is the volume fraction at which a continuous solids network is formed. β, n and p_a are fitting parameters that allow for fitting the equations to measured data.

Some other functional forms that have been suggested are [9,10]:

$$\phi = \phi_g \left(\frac{p_s}{p_a}\right)^{\beta}, \tag{4}$$

$$\phi = \phi_g \left[1 + \left(\frac{p_s}{p_a}\right)^{\beta}\right], \tag{5}$$

and

$$e = A - B \times \ln(p_s), \tag{6}$$

where $e = (1-\phi)/\phi$.

A more extensive listing of compressibility equations used in literature can be found in Olivier et al. [10].

Buscall and White [11] developed a unified theory of compressional rheology for the dewatering of flocculated suspensions. Key factors in this theory are the compressive yield stress $P_y(\phi)$ and the hindered settling factor $r(\phi)$. The latter relates the liquid velocity through the cake to the free settling velocity of the individual particles, while $P_y(\phi)$ is the pressure needed to collapse the cake irreversibly to a solids volume fraction ϕ. It can be shown that $r(\phi)$ is related to the specific resistance α [12,13]. Under the assumptions used in the further development of the theory [14–16], $P_y(\phi)$ is equivalent to $p_s(\phi)$. Buscall and White [11] regard these properties as material properties, rather than filtration properties and use their theoretical framework for settling and centrifugation as well as filtration.

Whereas most constitutive relationships were established empirically, Keiding and Rasmussen [2] suggested an interesting approach by interpreting the relationship between the solids volume fraction and the solids pressure in a more fundamental, physical way. They suggested that for slurries such as activated sludge, the osmotic pressure in the sludge matrix – due to the presence of charged polymeric substances – could be responsible for the high compressibility. They suggested that the solids pressure is equal to the osmotic pressure, and is given by

$$p_s = \sigma\rho\frac{\phi}{1-\phi}\mathcal{R}T, \tag{7}$$

with σ the charge density [eq/kg], ρ the solids density [kg/m^3], $\mathcal{R}$ the universal gas constant [J K^{-1} mole^{-1}] and T the temperature [K]. The authors found that this approach could reproduce the typical phenomenology of filtration dewatering of sludge.

Buscall and White [11] showed that the compressive yield stress function $P_y(\phi)$ (i.e. the constitutive equation) can be obtained from centrifuge experiments. They determined the final sediment bed height for different rotational speeds. Within their compressional rheology framework, they derived an approximate solution for P_y and ϕ at the bottom of the tube as a function of the centrifugal acceleration at the bottom of the tube. Green et al. [17] noted that it does not appear possible to show theoretically that this solution is

an accurate approximation for all functions of $P_y(\phi)$. Green et al. [17] suggested an iterative solution method, which includes numerically solving a set of differential equations. Again, this solution method yields values for P_y and ϕ at the bottom of the tube as a function of the centrifugal acceleration at the bottom of the tube.

In this work, we will develop a novel methodology for assessing the compressibility behaviour of particulate suspensions using the equilibrium sediment bed height during centrifugation. The relationship between solids pressure and solids volume fraction is obtained by parameter optimisation of a simple numerical model, based on straightforward physical principles. We will apply this methodology to an anaerobically digested sludge and we will assess various functional forms for the relationship between solids pressure and solids volume fraction at relatively low solids pressures. These pressures are relevant for gravity settling and centrifugation, and to a lesser extent for the filtration stage in pressure dewatering.

2. Materials and methods

2.1. Sludge

The sludge used for this work was a mesophilic anaerobically digested sludge from a waste water treatment plant at Carrum, Australia. During storage, biotic sludges tend to show a change in filtration behaviour due to the occurrence of biological processes. For activated sludge, it was seen that changes in extracellular polymeric substances slow down significantly towards the end of a 14-day storage period [18]. It was decided to use anaerobic sludge, and to keep it in a fridge (at 4 °C) for 14 days before use, to reduce the temporal variability. Although anaerobic sludges contain less organic material than aerobic sludges, they still possess a high compressibility and a low permeability, showing typical biotic sludge dewatering behaviour [19].

The sludge had a dry solids mass fraction of 1.7%, a pH of 7.33 and a conductivity of 6.25 mS/cm. The dry solids had a density of 1590 kg/m^3(based on the dry solids content and the densities of the sludge and the bulk liquid, corrected for dissolved solids). Dry solids volume fractions were calculated from the respective dry solids mass fractions and the dry solids densities. Preliminary centrifugation experiments showed that the sludge had a relatively high concentration of very small, hard to settle particles. This fraction would only settle at high centrifugation speeds, thus increasing the sediment bed height suddenly. This effect was strongly reduced by centrifuging the sludge in a Jouan CT422 refrigerated centrifuge (30 min, 3500 rpm), and resuspending 1 volume of the resulting sediment in 3 volumes of tapwater, yielding a sludge with a dry solids mass fraction of 1.0%, corresponding to a dry solids volume fraction of 0.63%. Note that changing the bulk liquid can result in a change of the sludge properties due to a change in the ionic equilibrium. Therefore, care has to be taken when applying this procedure while assessing the properties of a sludge, and these ion effects should be taken into account. Using gravity settling, the gel point was estimated to be 1.5% (w/w), which corresponds to a dry solids volume fraction of 0.95%. A sludge with a dry solids mass fraction of 2.0% (i.e., a dry solids volume fraction of 1.3%) was obtained by centrifuging the resuspended sludge again (90 min, 4000 rpm), decanting part of the supernatant and gently homogenising the remainder.

2.2. Centrifugation

A Lumifuge LF110 (Lum GmbH, Germany) was used for assessing the sediment bed height during centrifugation. The Lumifuge transmits light through the sample during the centrifugation, and a detector on the other side of the sample detects the light intensity as a function of the height in the sample. The sediment bed surface can be detected as a sharp decrease from high transmission to low transmission. A major advantage of this approach is that it allows for measurement of the bed height during the centrifugation process, whereas earlier methods often measured the bed height after the sample was removed from the centrifuge. For materials that exhibit some degree of elastic compressional behaviour, such as biotic sludges, this earlier technique is not indicative of the real bed height during centrifugation due to re-expansion of the bed. A more elaborate description of the apparatus can be found in Sobisch and Lerche [20].

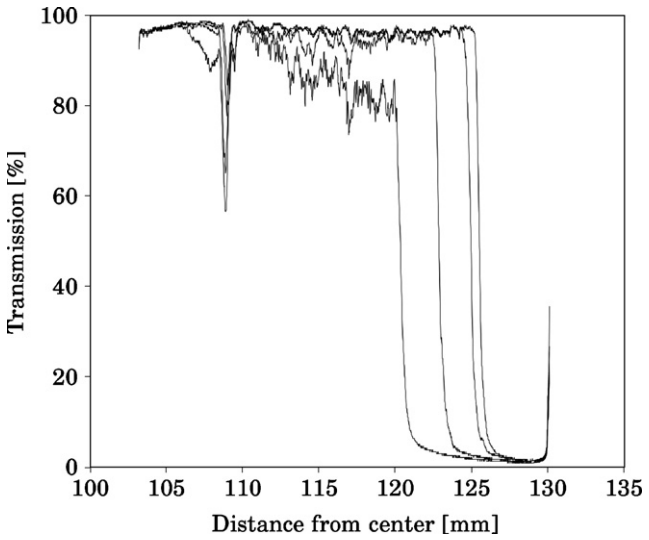

Fig. 1. The transmission profiles of a sample at the end of a period at constant speed. From left to right, the profiles are at 600, 1200, 2400 and 3000 rpm respectively.

The bottom of the sample tubes was at a distance of 0.130 m from the center of rotation. During the experiments, the rotational speed was increased stepwise. Due to software restrictions on the total operational time of the centrifuge, the maximum being around 42 h, two centrifugation schemes were used to span a rotational speed range from 300 to 3600 rpm. The first scheme applied 300, 900, 1800 and 3600 rpm during 700, 630, 600 and 600 min respectively, while the second scheme subjected the samples to 600, 1200, 2400 and 3000 rpm for the same periods of time. The time periods were chosen to generate as much data as possible within one run and within the software restrictions on the total time, while allowing the samples to approach equilibrium bed height as closely as possible. The temperature within the centrifuge was kept constant at 4 °C. Fig. 1 shows the transmission profiles of a sample at the end of each period at constant speed in the regime of 600, 1200, 2400 and 300 rpm. The profiles clearly show a sharp decrease in transmission, marking the surface of the sediment bed. The profile at 600 rpm shows a somewhat lower transmission in the supernatant (left side of the sharp decrease), indicating that a small amount of material is still left in the supernatant, due to the presence of very small particles, mentioned above.

The sample tubes were rectangular polycarbonate cells, supplied by Lum GmbH, with a cross-section of 0.002 m × 0.008 m. A volume of 350 μL was added to the sample tubes using a precision pipette, resulting in a suspension height of 0.022 m. The sediment bed height was determined as the position in the sample where transmission dropped below a threshold value of 40%. Fig. 2 displays the change of the sediment bed height as a function of time for a sludge sample with a 2.0% solids mass fraction subjected to the second centrifugation scheme. It shows that the bed height was close

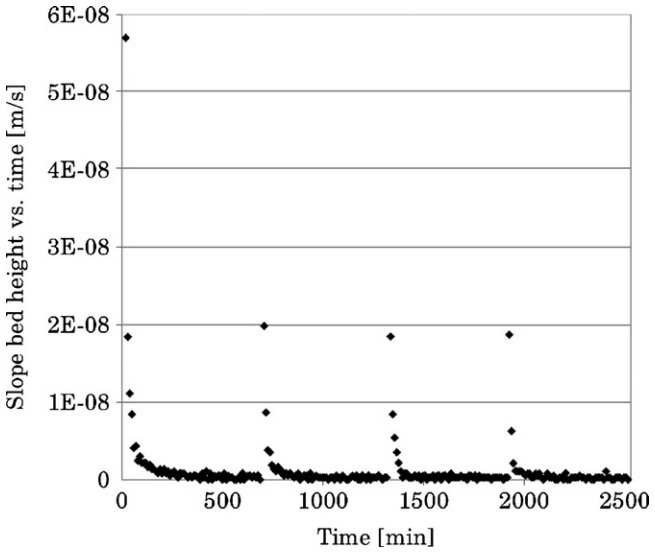

Fig. 2. The absolute value of the slope of the sediment bed height of a 2.0% (w/w) sludge sample as a function of time during a centrifugation regime of 700, 630, 600 and 600 min at 600, 1200, 2400 and 3000 rpm respectively.

to equilibrium before the rotational speed was stepped up. The sediment bed heights used for fitting and evaluating the model, were obtained by taking the average value of four different samples.

2.3. Parameter fitting

Fitting of the parameter values was done using a multi-dimensional non-linear minimisation (Nelder-Mead, Walters et al. [21]) of the sum of squared errors for different speeds. As this minimisation method searches for a local minimum starting from a given set of parameter values, different starting values were used when no satisfactory fit could be found.

3. One-dimensional equilibrium state centrifugation model

The centrifugal force is a reactive force, acting in the radial direction. It is convenient to depict centrifugation using a rotating frame of reference, with its origin in the centre of the centrifuge and with the same angular speed as the centrifugation itself, as shown in Fig. 3. The bottom figure shows a scaled representation of the real dimensions of the sediment bed in the centrifuge. During centrifugation at an angular speed of ω, the centrifugal force F_c acting on a particle along the X-axis, at a distance R from the origin obeys:

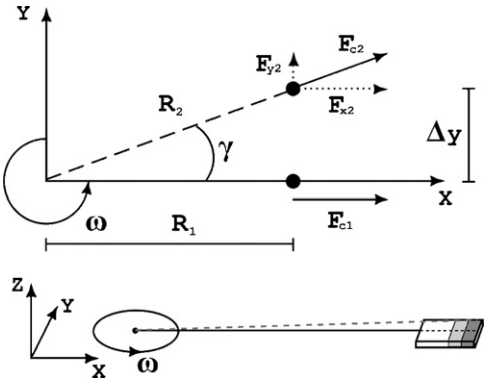

Fig. 3. The upper figure shows a schematic two-dimensional representation of centrifugation. The bottom figure shows a three- dimensional scaled representation of the sediment bed in the sample at the start (white), at 600 rpm (light grey) and at 3000 rpm (dark grey).

$$F_c = m \times a, \tag{8}$$

$$F_c = m \times \omega^2 \times R, \tag{9}$$

with m the mass of the particle [kg], a the acceleration [m/s^2] and ω the angular speed of the centrifugation [rad/s]. When the particle is submerged in a liquid, this becomes:

$$F_c = V \times \Delta\rho \times \omega^2 \times R, \tag{10}$$

where V is the volume of the particle [m^3], and $\Delta\rho = (\rho_{sol} - \rho_{liq})$ is the difference between the density of the solid particle and the liquid respectively [kg/m^3].

Considering a layer of thickness dR at a radial distance R, the particles in this layer exert a downward force equal to:

$$dF_c = \phi \times dV \times \Delta\rho \times \omega^2 \times R, \tag{11}$$

$$dF_c = \phi \times dR \times S \times \Delta\rho \times \omega^2 \times R, \tag{12}$$

with ϕ the solids volume fraction in that layer, dV the total volume of the layer, and S the surface area of the layer. Hence, the force per unit area (i.e., the solids pressure) corresponds to:

$$dp_s = \frac{dF_c}{S} = \phi \times dR \times \Delta\rho \times \omega^2 \times R. \tag{13}$$

3.1. Assumptions

In this work, we use an algorithm that calculates the equilibrium sediment bed height as a function of the rotational speed, based on the constitutive relationship between porosity and solids pressure. Whereas in reality, the forces acting on the sample are acting along three dimensions, the numerical model used in this work only considers the main force during centrifugation, directed along the X-axis.

As shown in Fig. 3, the centrifugal force F_{c2} on a particle that is not positioned on the X-axis consists of a component along the X-axis and a component along the Y-axis. The component along the X-axis F_{x2} is equal to:

$$F_{x2} = \cos(\gamma) \times F_{c2} = \frac{R_1}{\sqrt{R_1^2 + \Delta^2 y}} \times F_{c2}. \tag{14}$$

The Y-component is equal to:

$$F_{y2} = \sin(\gamma) \times F_{c2} = \frac{\Delta y}{\sqrt{R_1^2 + \Delta^2 y}} \times F_{c2}. \tag{15}$$

For any particle within the sample, however, the X-component is equal to the centrifugal force acting on a particle along the X-axis at the same height in the sample:

$$F_{x2} = m \times \cos(\gamma) \times R_2 \times \omega^2 \tag{16}$$

$$F_{x2} = m \times \cos(\gamma) \times \frac{R_1}{\cos(\gamma)} \times \omega^2 = F_{c1}. \tag{17}$$

This means that particles at a certain height in the sample experience the same force along the X-axis, irrespective of their Euclidean distance from the X-axis.

A one-dimensional centrifugation model does not take into account the Y-component. In reality, this Y-component acts perpendicular to the wall of the container, and could increase the effect of friction. Eqs. (14) and (15) show that the ratio of the Y-component to the X-component is equal to $\Delta y/R$. In our setup, the maximum value for this ratio is 0.037. The error is further reduced by the fact that the sediment bed height is measured in the middle of the sediment bed width, i.e. along the X-axis. At this position,

the centrifugal force consists of only an X-component, and friction effects are reduced by the distance from the walls.

The influence of gravity is neglected based on the fact that it acts perpendicular to the centrifugal plane (and hence perpendicular to the observed change in sediment bed height), that in total, less mass is present in the Y-direction than in the X-direction and that the gravitational acceleration is much smaller than the centrifugal acceleration (a ratio of less than 0.02 on the bottom of the tube at 600 rpm).

Potentially the major source of error due to treating the centrifugation as purely one-dimensional is introduced by the radial dilution effect. As particles move radially away from the center, the interparticle distance increases, resulting in a dilution. In a rectangular sample tube, this effect will be counteracted by its walls. Once a particle network is formed, the lateral displacement turns into a lateral compression of the sediment. As shown above, this is negligible with respect to the compression in the X-direction. As it is counteracted by the formation of a network, this effect can be expected to be more important for highly diluted systems. There was no experimental evidence for a major influence of the dilution effect in any of the experiments performed within the scope of this work.

3.2. Calculating equilibrium bed height

Using Eq. (9), one can calculate the centrifugal acceleration at each height in the sample. It is hard, however, to calculate the equilibrium volume fraction profile directly. At each position in the sample, the solids pressure, and hence the solids volume fraction, is determined by the cumulative force generated by the particles higher in the sample. However, the total force these particles generate depends on the solids volume fraction lower in the sample. In a more compressed sediment, the particles are at a larger distance from the center of rotation, which results in a higher total particle pressure. Hence, compression results in a higher total solids stress, resulting in more compression, resulting in a higher solids stress again. The easiest way to solve this problem is using an iterative numerical approach, searching for the solids volume fraction distribution that implies an equilibrium between the solids pressure (as calculated according to one of the constitutive equations mentioned above) and the total pressure induced by the particles higher in the sample (calculated according to Eq. (13)). When using Eq. (2) as the constitutive equation, it searches for a solids distribution $\phi(R)$ that satisfies for each position R_i in the sample:

$$\int_{R_{top}}^{R_i} \phi(R) \times \Delta\rho \times \omega^2 \times R \, dR = p_a \left[\left(\frac{\phi(R_i)}{\phi_g} \right)^{(1/\beta)} - 1 \right] = p_s, \quad (18)$$

with R_{top} the distance between the top of the sediment bed and the rotational center. A detailed explanation of the algorithm used in this work is given in Appendix A.

Given that the errors from the one-dimensional approach are relatively small, and that the physics behind the equilibrium state in centrifugation are simple and well understood, the main source of error and uncertainty is the constitutive equation relating solids pressure to solids volume fraction. As such, equilibrium bed height centrifugation is ideal for assessing the validity of different functional forms for the constitutive equation at relatively low pressures. Furthermore, at a given rotational speed, a relatively broad range of compressive pressures is generated within the sediment bed, a range that can be extended even further by changing the rotational speed. The method provides a convenient way of estimating the parameter values, once a specific functional form has been chosen.

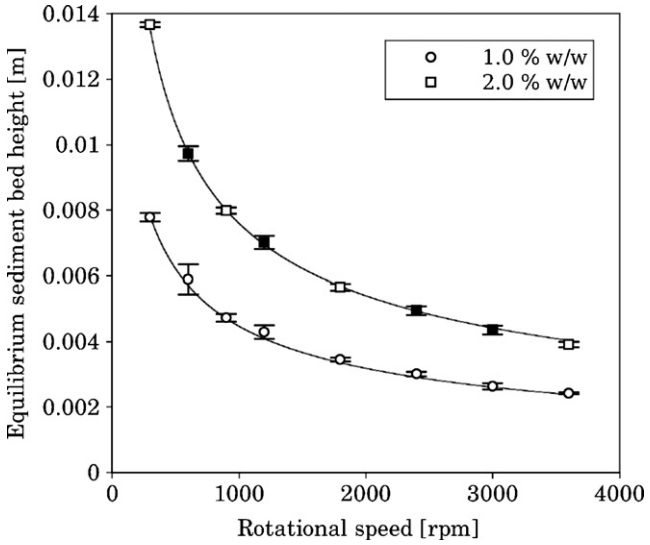

Fig. 4. Sediment bed height as a function of rotational speed for samples with a sample height of 0.022 m and a solids mass fraction of 0.01 and 0.02 respectively. Symbols are measured values; filled symbols were used for estimation of the values of the parameters p_a and β, whereas the solid lines represent model predicted values.

4. Results

4.1. Fitting

To assess the validity of the model, samples with two different solids mass fractions (i.e. 1.0 and 2.0%, w/w) were centrifuged. Eq. (2) was used as the constitutive equation in the model; the other equations will be discussed later. The density of water at the operational temperature (i.e. 1000 kg/m^3) was selected for the liquid density (ρ_{liq}), whereas a value of 1590 kg/m^3 was assumed for the solids density (ρ_{sol}). Assuming that the water which is removed from the sludge during the determination of the dry solids content has the same density as the bulk liquid, the water itself does not generate a net force. As such, the volume and density of the real dispersed phase can be replaced with the volume and density of the dried solids. The gel point volume fraction ϕ_g was set to 0.95%. The measured bed heights for the samples with the highest mass fraction at rotational speeds of 600, 1200, 2400 and 3000 rpm were used for fitting the parameter values p_a and β. This resulted in a value of 0.3042 Pa for p_a and 0.2462 for β. These parameter values were then used to predict the bed height at all speeds, and for different initial solids fractions.

Fig. 4 shows the equilibrium sediment bed height as a function of rotational speed for the two mass fractions. Fig. 5 shows the experimental average solids volume fraction in the sediment for the different speeds. These values were calculated using the initial bed height, the initial solids volume fraction and the final bed height. A higher initial solids concentration results in a higher solids volume fraction in the sediment due to the increased cumulative compressive force. This effect is clearly stronger than the decrease in the average distance from the centre (which, according to Eq. (9), decreases the centrifugal force). The symbols in Fig. 4 represent the average measured bed heights, the error bars show the standard deviation. The black squares show which values were used for fitting the parameter values. The solid lines show model predictions for the total experimental range of speeds, and the two different initial solids mass fractions. The figure clearly shows that the numerical algorithm, in combination with the functional form of Eq. (2), is very well capable of modelling the sediment bed height as a function of rotational speed. For a given solids mass fraction,

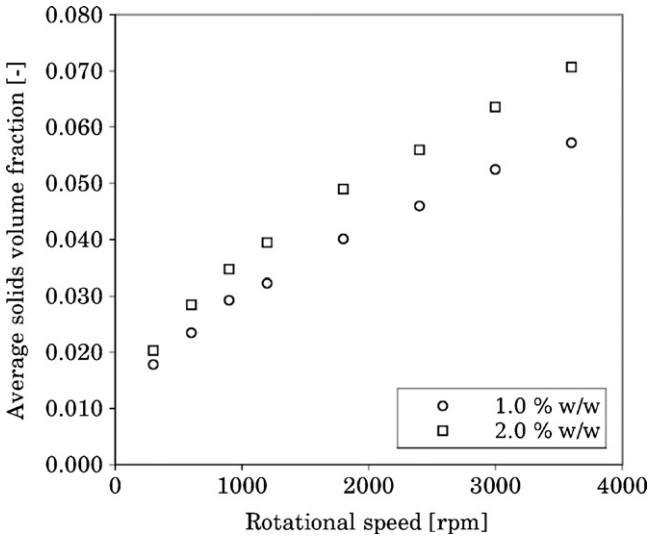

Fig. 5. The experimental mean solids volume fractions over the total sediment bed as a function of rotational speed for samples with a sample height of 0.022 m and a solids mass fraction of 0.01 and 0.02 respectively.

the model not only interpolates well, but it performs good as well at extrapolating to rotational speeds outside the experimental range and to different initial solids concentrations. The good results for the extrapolations are partly contributed to the fact that during centrifugation, the solids are subjected to a range of solids pressures instead of one particular pressure.

Fig. 6 gives an overview of the sensitivity of the fitting parameters. It shows the relative change in the sum of squared errors, which is minimised during fitting, as a function of a relative change in the parameter values. The figure shows that β is a sensitive parameter (note the scale difference between the two axes). A deviation of 1.0% from the optimum value of β without changing the value of p_a induces an increase in the sum of squared errors of more than 350%. p_a is less sensitive, but a deviation of 1.0% from its optimum value still induces an increase of more than 11% in the sum of squared errors.

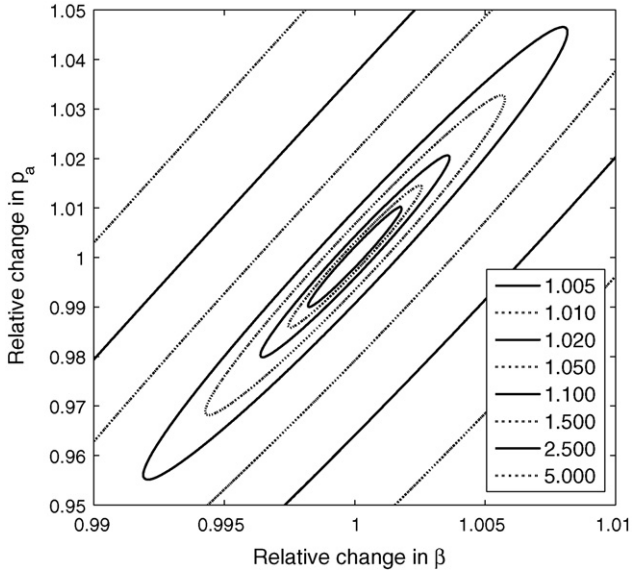

Fig. 6. A contour plot of the relative change in the optimisation criterion (sum of squared errors) with regard to the optimum value as a function of relative change in the parameter value. The lines depict parameter combinations that yield the same sum of squared errors. The values for the relative change of the SSE, starting from the center, are shown in the legend.

Table 1
The parameter fitting results for different assumed values for the solids density, with ϕ_g fixed at 0.95%.

Parameter	$\rho = 1490$ kg/m^3	$\rho = 1590$ kg/m^3	$\rho = 1690$ kg/m^3
p_a [Pa]	0.26965	0.30419	0.33466
β	0.24618	0.24618	0.24617

4.2. Solids density

Eq. (10) shows that the centrifugal force generated by the solids depends on the density difference between the solids and the liquids. It is important to note, however, that with regard to average solids volume fractions, the functional form of Eq. (2) is more or less insensitive to errors in the solids density. When fitting the model with different values for the solids density, the resulting values for the parameters in Eq. (2) will be different, but the resulting calculated sediment bed heights will be the same. This is due to the change in parameter values compensating for the change in the solids density. Table 1 shows the parameter fitting results for different values for the solids density, using Eq. (2) as the constitutive equation. This means that for predicting final average volume fractions, the exact value for the solids density is not crucial when using Eq. (2). However, the use of an incorrect solids density will result in incorrect solids pressure profiles. Hence, a good approximation of the solids density is still desirable. For the gel point ϕ_g, an estimated parameter as well, a similar behaviour was seen, where a small difference in the set value yielded a comparable fitting performance.

Assuming a solids density of 1590 kg/m^3, Fig. 7 shows the solids pressure profile and the solids volume fraction as a function of height in the sediment bed for two sludge samples with an initial height of 0.022 m, a solids mass fraction of 1.0 and 2.0% (w/w) respectively, and at a rotational speed of 3600 rpm.

4.3. Other constitutive equations

The analysis using Eq. (2) yields good results for fitting and predicting equilibrium bed height. Table 2 shows R^2 values for the

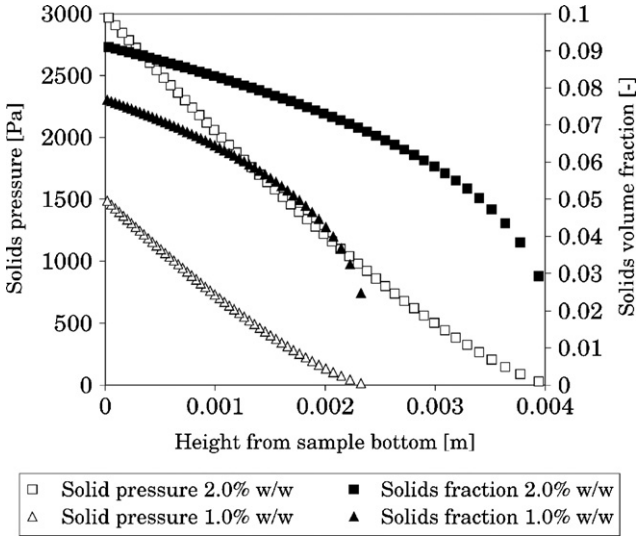

Fig. 7. The solids pressure profile and the solids volume fraction as a function of height in the sediment bed for two sludge samples with a solids mass fraction of 1.0 and 2.0% (w/w) respectively, and at a rotational speed of 3600 rpm

Table 2
Parameter values yielding the best fit for the different functional forms and R^2 values for the resulting fits.

Functional form	Param. 1	Param. 2	$R^2_{0.01}$	$R^2_{0.02}$
Eq. (2)	$p_a = 0.3042$	$\beta = 0.2462$	0.9954	0.9995
Eq. (7)	$\sigma\rho RT = 525.6$	–	−95.03	−23.05
Eq. (4)	$p_a = 0.2803$	$\beta = 0.2434$	0.9928	0.9995
Eq. (5)	$p_a = 3.295$	$\beta = 0.3274$	0.9765	0.9902
Eq. (6)	$A = 53.34$	$B = 5.900$	0.9104	0.9534
Eq. (20)	$\sigma\rho RT = 14.56$	$b = 17.15$	0.2286	0.9092

other functional forms mentioned in Section 1. R^2 values are not the optimal goodness-of-fit indicators for non-linear equations, but for different fits to the same data set, they present an easily interpretable scaled version of the squared errors. R^2 values were calculated according to:

$$R^2 = 1 - \frac{\mathrm{SSE_{fit}}}{\mathrm{SSE_{mean}}}, \tag{19}$$

with $\mathrm{SSE_{mean}}$ and $\mathrm{SSE_{fit}}$ the sum of squared errors calculated relative to the average measured value and the predicted values respectively. For fitting the parameter values, the bed heights at 600, 1200, 2400 and 3000 rpm for the 0.02 mass fraction samples were used. R^2 values were calculated using the measured bed heights at all speeds for both solids mass fractions. Negative R^2 values indicate that the average value yields a lower sum of squared errors than the best fitting model prediction.

Table 2 indicates that Eq. (2), the constitutive equation that is most used in filtration modelling, also yields the best fit for centrifugation. Eqs. (4) and (5) yield reasonably good fits as well. The resulting modelled sediment bed heights for both functions suggest that the biggest deviation appears at lower pressures (data not shown). Eq. (6) results in a significantly worse fit, and Eq. (7) can not be fitted to the measured values at all. Eq. (7) however, is very dependent on the assumed value of the solids density, due to its specific form. To allow for the functional form to compensate for an incorrect solids volume fraction, Eq. (7) can be adapted to:

$$p_s = \sigma\rho\frac{b\phi}{1-b\phi}RT. \tag{20}$$

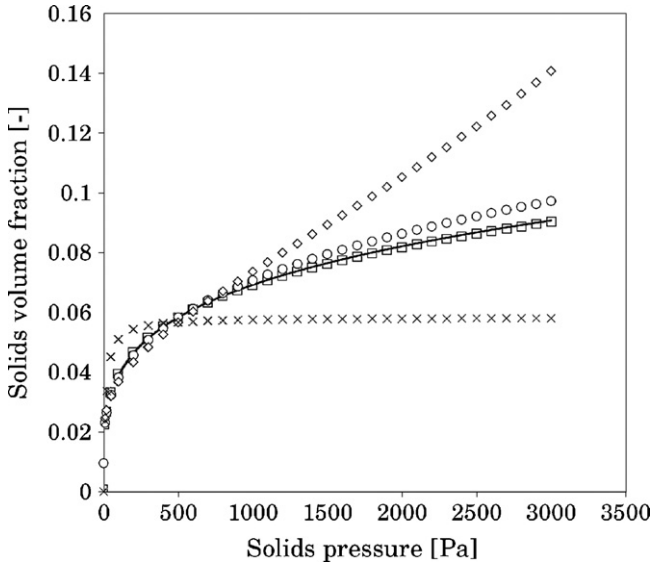

Fig. 8. The solids volume fraction as a function of the solids pressure according to the different functional forms. The solid line depicts Eq. (2), □Eq. (4), ○Eq. (5), ◊Eq. (6) and × Eq. (20).

This yields slightly better results, as shown in Table 2, but still the fit is not satisfactory. Furthermore, the fitted value for the correction factor is too high to be realistic. This seems to indicate that the osmotic pressure alone cannot account for the total solids pressure, and that the solids pressure for a significant part due to another, structural resistance against compression.

Fig. 8 shows the predicted solids volume fractions as a function of the solids pressure as calculated by the different functional forms mentioned above. Eqs. (2) and (4), which result in the best fit, show a very similar relationship between solids pressure and solids volume fraction after parameter fitting. The more the other equations deviate from this relationship, the less accurate the fit becomes.

5. Conclusions

It was shown that a relatively simple numerical model can predict the equilibrium sediment bed height as a function of rotational speed during centrifugation. The advantages over previous methods are the direct measurement of the sediment bed height during filtration, and the relative ease of implementation due to the use of straightforward mathematical and physical principles. Different functional forms for the relationship between solids pressure and solids volume fraction – typically used for describing filtration behaviour – were compared with respect to their ability to describe compressibility during centrifugation. The functional form suggested by Tiller and Leu [1] resulted in the best predictions. A relationship based on the osmotic pressure alone is not able to yield good predictions of actual sediment bed heights during centrifugation. This suggests that the osmotic pressure alone cannot account for the total solids stress, and that a structural resistance to compression should be considered as well.

The approach demonstrated in this work, forms an easy way of assessing the low pressure compressibility of a biotic sludge or any other compressible material. The results from this assessment can be used for modelling purposes in gravity settling and centrifugation. When applying the results to pressure dewatering, it is of major importance that the particle density is known. Furthermore, the results of this assessment can only be used for particle pressures within the range reached during the centrifugation experiments. As such, compression experiments at higher pressures are still required to cover the total range of solids pressures relevant to pressure dewatering.

Acknowledgements

One of us, D. Curvers, acknowledges the financial support he receives from FWO Vlaanderen (Scientific Research Fund of Flanders) as an aspirant of FWO. He is also greatly indebted to D. Huygens and P. Saveyn for invaluable discussions. Further funding assistance for the work was from the Particulate Fluids Processing Centre, a Special Research centre of the Australian Research Council.

Appendix A. Numerical algorithm

In contrast to, e.g. gravity, the centrifugal acceleration is not constant throughout the sample. When particles closer to the bottom get more compressed, the rotational radius for the particles higher in the sample gets larger, and the force they exert on the lower particles gets larger as well, which in turn compresses the lower particles further again, and so on. This process continues until an equilibrium is reached where for any height in the sample, a solids fraction is reached with a solids pressure that equals (and counteracts) the total force exerted by the particles higher in the sample.

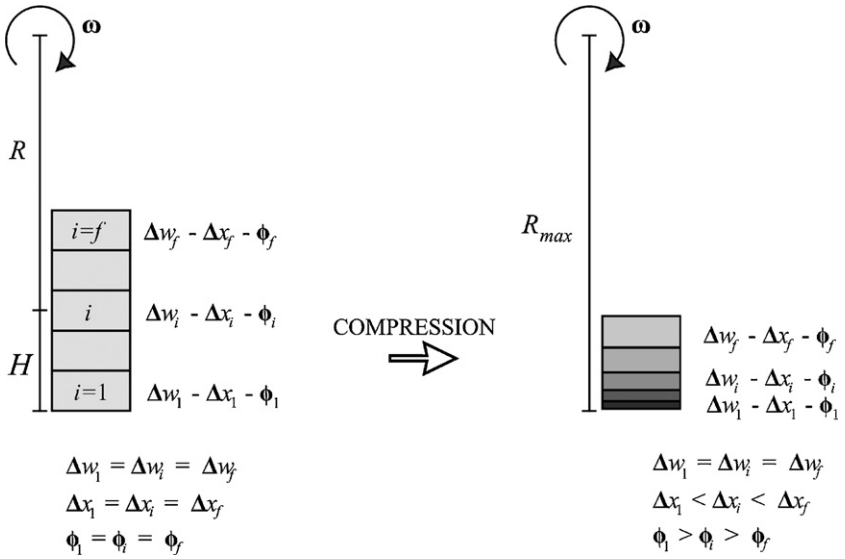

Fig. A.1. Schematic presentation of the material coordinate. As the sediment gets compressed, the different volume fractions ϕ_i increase, and the layer thicknesses Δx_i decrease, but Δw remains constant.

This equilibrium solids fraction profile can be calculated using an iterative algorithm.

Defining a one-dimensional material coordinate simplifies the calculation. We define a given position w_i as the total volume of solids between that position and the bottom of the tube divided by the cross-section area. The top of the sediment is at $w = w_{tot}$, while the bottom is at $w = 0$. The total amount of solids, w_{tot} is divided in f finite differences $\Delta w_i = w_{tot}/f$. The advantage of a material coordinate is that the position of a given particle does not change when the solids volume fraction increases, so Δw_i does not change during compression, as shown in Fig. A.1. Furthermore, the material coordinate system removes the moving boundary of the sediment bed surface, greatly simplifying the calculations.

Fig. A.2 shows a flow chart of the algorithm. Initially, the solids volume fraction is assumed to be constant throughout the sample. The algorithm starts by calculating the size of Δw_i of the separate layers. The thickness of each layer in absolute space coordinates Δx_i is calculated as $\Delta x_i = \Delta w_i/\phi_i$. For each layer, its height within the sample (relative to the bottom), H_i, is equal to the sum of the thicknesses Δx_j of the lower layers plus half of its own thickness. The rotational radius R_i is equal to $(R_{max} - H_i)$, with R_{max} the maximum radius (at the bottom of the tube). Using the rotational radius, one can calculate the increase in solids pressure each layer contributes to the layers lower in the sample according to Eq. (10). The total solids pressure in a layer is equal to the sum of the contributions from all the layers higher in the sample. Using the constitutive equation, this pressure can be related to a new solids volume fraction ϕ_i for each Δw_i, taking into account that the solids volume fraction can not be lower than the initial solids volume fraction. With this new ϕ_i, a new Δx_i can be calculated, resulting in a new net force for each Δw_i, and so on. This loop is repeated until the difference in the total bed height is smaller than a predefined threshold value.

This algorithm is not intrinsically stable. Theoretically, it is possible that for a certain set of parameter values and bound-

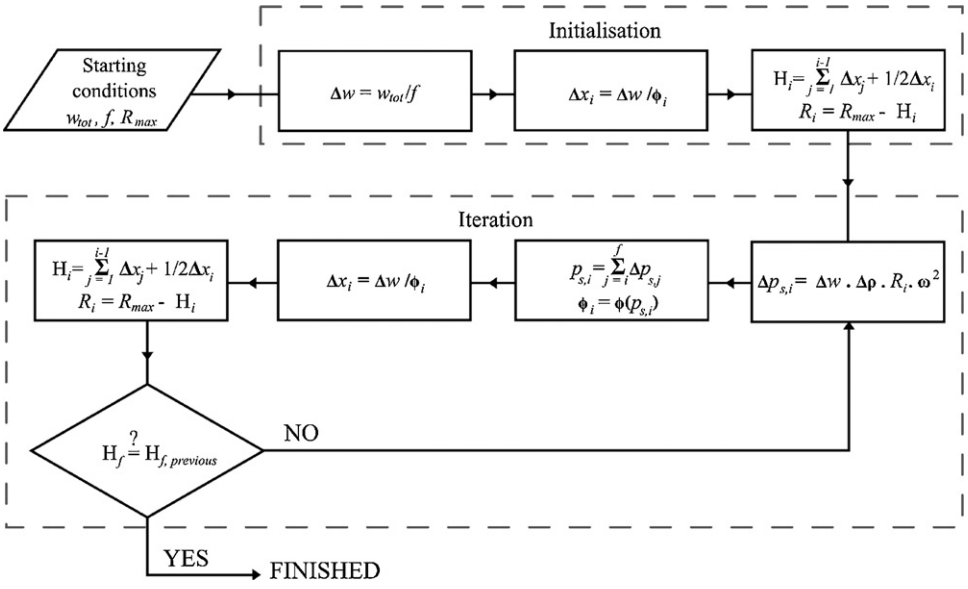

Fig. A.2. Flow chart for the algorithm used for calculating the equilibrium sediment bed height.

ary conditions, the algorithm starts oscillating around the 'real' solution. Neither does this algorithm guarantee that the resulting solution is a physically meaningful solution. This can easily be checked however, by looking at the resulting solids volume fraction or solids pressure profile. Under the conditions tested for this work, the algorithm always converged relatively fast ($\leq$ 10 iterations for a relative error smaller than $1e^{-15}$), and yielded meaningful solutions.

References

[1] F. Tiller, W. Leu, Basic data fitting in filtration, Journal of the Chinese Institute of Chemical Engineers 11 (1980) 61–70.
[2] K. Keiding, M. Rasmussen, Osmotic effects in sludge dewatering, Advances in Environmental Research 7 (2003) 641–645.
[3] G. Tchobanoglous, F. Burton, Wastewater engineering treatment, disposal and reuse, 3rd edition, Metcalf & Eddy Inc., New York, 1991.
[4] R. Wakeman, Separation technologies for sludge dewatering, Journal of Hazardous Materials 144 (2007) 614–619.
[5] B. Ruth, G. Montillon, R. Montonna, Studies in filtration. 1. Critical analysis of filtration theory, Industrial and Engineering Chemistry 25 (1933) 76–82.
[6] B. Ruth, G. Montillon, R. Montonna, Studies in filtration. 2. Fundamental axiom of constant-pressure filtration, Industrial and Engineering Chemistry 25 (1933) 153–161.
[7] P. Sorensen, J. Hansen, Extreme solid compressibility in biological sludge dewatering, Water Science and Technology 28 (1993) 133–143.
[8] J. Novak, M. Agerbaek, B. Sorensen, J. Hansen, Conditioning, filtering, and expressing waste activated sludge, Journal of Environmental Engineering 125 (1999) 816–824.
[9] K. Landman, L. White, R. Buscall, The continuous-flow gravity thickener—steady-state behavior, AIChE Journal 34 (2) (1988) 239–252.
[10] J. Olivier, J. Vaxelaire, E. Vorobiev, Modelling of cake filtration: an overview, Separation Science and Technology 42 (2007) 1667–1700.
[11] R. Buscall, L. White, The consolidation of concentrated suspensions. 1. The theory of sedimentation, Journal of the Chemical Society—Faraday Transactions I 83 (1987) 873–891.
[12] M. Green, Characterisation of suspensions in settling and compression, Ph.D. thesis, Department of Chemical Engineering, The University of Melbourne (1997).
[13] R. de Kretser, P. Scales, Linking dewatering parameters from traditional, fluid mechanical and geotechnical theories, Filtration 7 (2007) 60–66.
[14] K. Landman, L. White, Determination of the hindered settling factor for flocculated suspensions, AIChE Journal 38 (1992) 184–192.
[15] K. Landman, L. White, Solid/liquid separation of flocculated suspensions, Advances in Colloid and Interface Science 51 (1994) 175–246.
[16] K. Landman, L. White, Predicting filtration time and maximizing throughput in a pressure filter, AIChE Journal 43 (1997) 3147–3160.
[17] M. Green, M. Eberl, K. Landman, Compressive yield stress of flocculated suspensions: determination via experiment, AIChE Journal 42 (1996) 2308–2318.
[18] P. Nielsen, B. Frolund, K. Keiding, Changes in the composition of extracellular polymeric substances in activated sludge during anaerobic storage, Applied microbiology and biotechnology 44 (6) (1996) 823–830.
[19] A. Ayol, A. Filibeli, S. Dentel, Evaluation of conditioning responses of thermophilic–mesophilic anaerobically and mesophilic aerobically digested biosolids using rheological properties, Water Science and Technology 54 (2006) 23–31.
[20] T. Sobisch, D. Lerche, Application of a new separation analyzer for the characterization of dispersions stabilized with clay derivatives, Colloid and Polymer Science 278 (2000) 369–374.
[21] F. Walters, L.J. Parker, S. Morgan, S. Deming, Sequential Simplex Optimization: A Technique for Improving Quality and Productivity in Research, Development, and Manufacturing, CRC Press, Boca Raton, 1991.